BACHELOR THESIS

Characterizing α-Synuclein Polymorphs Through AFM, SAA, Spectrophotometry and Digestion Assay

W. Chen

Biomedical Technology

Faculty of Science and Technology

University of Twente

Committee Chair: Prof. Dr. M.M.A.E. Claessens
Daily Advisor: Dr. Ir. S.A. Semerdhziev
External Member: S.S.M.C. Michel-Souzy

16th of July 2024

Abstract

SAAs have made it possible to detect PD by being able to identify α-synuclein aggregations. Currently, researchers are working on finding out how polymorphs affect SAAs, as well as on how they affect synucleinopathies. This report will emphasize on finding discriminatory properties of different strains first and will serve as a stepping stone for the previous mentioned research purposes. To begin with, according the amplification rates were significantly different between the polymorphs. In addition, through AFM it has been found that although height does not differ among the strains, periodicity does. Furthermore, some strains produced unique spectra in the spectrophotometer when using the dyes ThT, Amy, ANS and NR, implying differences in how well each strain binds to the dye, which is influenced by the structure of the strain. Lastly, no conclusion could be drawn from the results of the proteinase K digestion, as the experiment was not successfully executed. Overall, some unique properties of strains have been found through these methods.

Keywords: α-synuclein, Parkinson's disease, amyloid, WT, ribbons, fibrils, A53T, E46K, SAA, AFM, spectrophotometry, digestion assay

1 Introduction

Parkinson's Disease (PD) is one of the most common age-related motoric neurodegenerative diseases[1]. Symptoms include tremor, muscle stiffness, slowness of movement, and impaired balance. Typically, the condition starts to develop at 60 years due to genetic reasons as well as sporadic. Furthermore, it is estimated that 1% of people over 60 have this condition, it being 1.8x more common in men than in women. No cure has been found yet for PD, but there are some therapies and medicine that alleviate the symptoms[2] Detection for PD is currently based on subjective clinical assessments, and there are no conclusive and certain methods for this on the market yet. In recent developments, however, the presence of α-synuclein (αS) aggregates have been discovered in the bodily fluids of patients with PD, like blood, cerebral spinal fluid, and saliva, as well as other tissues, like skin[3]. These can be detected through a Seed Amplification Assay (SAA), which originally was used for prion detection, but the technique turned out to work for other amyloids as well[4].

As mentioned before, diagnosing PD relies on subjective clinical assessments, like medical history and neurological examinations[1]. These can lead to misdiagnosis or delayed diagnosis. There is also no recommended biomarker-based test on the market for clinical use for diagnosis, only for ruling out other diseases that are similar to PD, like blood tests and imaging techniques[2]. This makes early and accurate detection challenging. As a result, treatment is delayed and may end up less effective for a specific type of PD.

SAAs, on the other hand, show a sensitivity and specificity of 87.7% and 96.3% respectively[5]. This may vary per type of aggregate. A type of aggregate is also called a polymorph or strain. What determines the type lies in changes in the environment, as they influence the formation of the protein. Characteristics of polymorphs may influence how efficiently the αS aggregates are detected through the SAA, as those with glucocerebrosidase (GBA) PD, stemming from a mutation in the GBA gene, were more likely to be positive in SAA than sporadic, which is caused by multiple genetic and environmental factors[6,7]. Even less likely to be tested positive were those with a gene mutation on leucine-rich repeat kinase 2 (LRRK2)[5]. Additionally, having an olfactory deficit, an inability to identify odors, led to being more likely to be tested positive. In other words, previous research has found a relationship between the result of an SAA and polymorph.

The mutations A53T and E46K cause an increase in propensity to form fibrils, A53T more than E46K, which is in line with the age of disease onset, respectively being 60 and 45 years[8]. Additionally, previous research has shown that fibrils, WT aggregates formed in high salt (HS) conditions, amplify faster and therefore reach a plateau faster than ribbons, WT aggregates formed in low salt (LS) conditions, do in an SAA[9,10]. In addition, fibrils have a higher tendency to bind and penetrate cells and are also more toxic than ribbons[9]. This suggests that the type of polymorph influences some parts of a synucleinopathy, in this case the severity and progression rate.

Taking into account that there is a detectable difference between the mutants and between the WT aggregates in an SAA and also maintain some relationship with the severity and rate of a neurodegenerative disorder, it may be the case that different synucleinopathies can be uniquely characterized through this diagnostic technique, as various strains of αS may appear significantly different in terms of amplification rate.

It is thus important to investigate how these differences may affect SAAs and lead to discrimination between different synucleinopathies. For that, differences in properties of polymorphs will be analyzed through various methods. The polymorphs that will be discussed are: (sonicated) wild-type (WT), ribbons, fibrils, E46K, and A53T. If diagnoses that specify disease type and stage can be made, this can lead to more targeted therapy and a better quality of life for patients with PD.

2 Theoretical Background

2.1 α-Synuclein Aggregation

During PD, α-synuclein, a protein made of 140 amino acids, consisting of six repeats and mainly found in neurons, aggregates[8]. The process is visualized in Figure 1. αS monomers that are already present in the body will form a small aggregate, also called an oligomer[3,11]. This process is called primary nucleation. Primary nucleation is more likely to happen when there are metal ions, micromolecules, gene mutation or post-translational modification of the protein present. The oligomer will first grow by elongation, where monomers attach to the ends. The assembling of this will result into compact β-sheet structures, which are characteristic for amyloid fibrils. After, amyloids can now also grow by secondary nucleation. This process involves monomers interacting with the surface of the formed fibrils, forming new oligomers. These oligomers can grow into fibrils as well. As this process repeats itself, eventually an amyloid body like a Lewy body or neurite will be formed. It is also possible that fragmentation occurs, where split into shorter fibrils. In practice, a combination of elongation, secondary nucleation and fragmentation of fibrils take place.[11,12]

In healthy individuals, αS is suggested to involve synaptic transmission[8]. Though the exact mechanism remains unknown, dopaminergic neurons degrade because of the αS aggregates. The aggregates also have a cytotoxic effect on cells by affecting proteins that function in many cellular processes. It can, for example, interfere with the Ubiquitin/Proteasome System (UPS), a regulated mechanism of intracellular protein

degradation and turnover. This could be one of the pathways that factor into the neurodegeneration mentioned above[3].

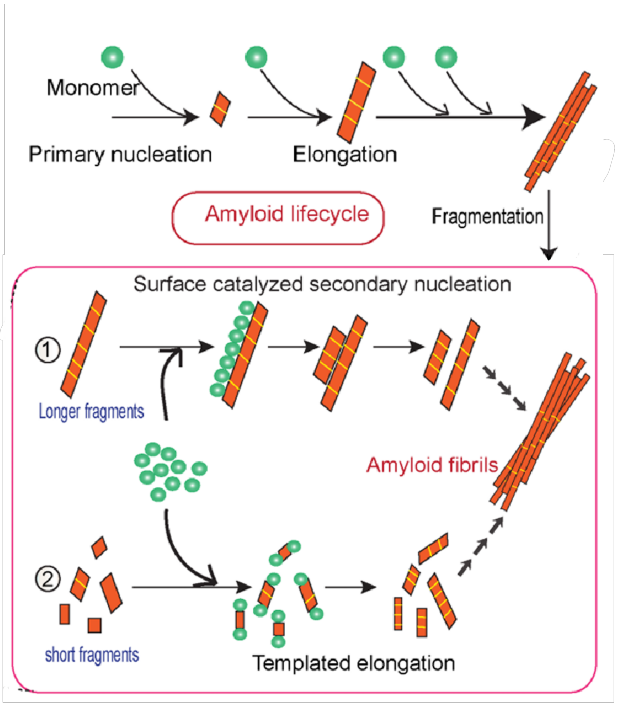

Figure 1 Simplified model of the aggregation process.[11]

2.2 Seed Amplification Assay

SAA makes use of the aggregation process. They involve, as the name suggests, a mixture of preformed aggregates, called seeds, as well as monomers. These are shaken at a controlled temperature to promote amplification, as fibrils and monomers can more easily come into contact with each other, as well as to create a homogenous distribution for fluorescence measurements. As monomers come into contact with the seeds, more fibrils will form. If stained with Thioflavin T (ThT), a dye that will be elaborated on in Section 2.6, the kinetics of the aggregation can be measured through a plate reader. The kinetics will be expressed as fluorescence over time.

If fluorescence increases, it means the amyloid mass has increased. As the amplification assay finishes, an S-shaped curve can be formed, see Figure 2. The curve can then be characterized by lag time. The lag time is the duration of plateau, which is the flat beginning of the graph. If amplification is instant, there is no lag phase and the curve will start at the elongation phase. In this case, one can choose to determine the slope, which is in this context the rate at which the fluorescence increases. It can be calculated by drawing a tangent that closely follows the curve and choosing two points on that line, then dividing the difference found in fluorescence by the difference in time, see Figure 3. For the initial slope, the same is done, except the points chosen are at and near the origin. The last phase of an SAA starts when the fluorescence will reach a maximum in the plateau phase, because either there are no more monomers to attach to the seeds, no more dye to bind to it or no more space on the seed for the dye to bind to.

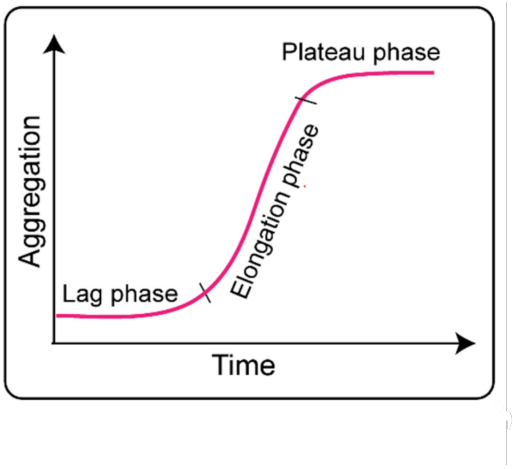

Figure 2 Example of an S-curve in red. This is generally what an SAA looks like. The blue curve represents the controls, where no aggregation takes place.[12]

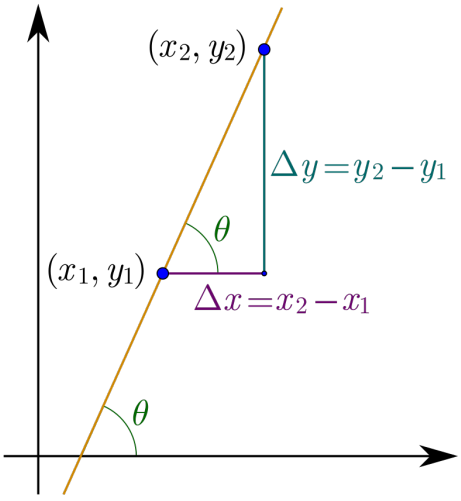

Figure 3 Visual aid with how a slope can be determined.[13]

2.3 Synucleinopathies and Polymorphs

A synucleinopathy is a type of degenerative disorder involving αS aggregation. The three most common synucleinopathies are PD, dementia with Lewy bodies (DLB), and multiple system atrophy (MSA)[14]. Types of αS aggregates defined by morphological differences are called polymorphs or strains.

The strains ribbons and fibrils are both formed of WT αS monomers. Ribbons are described as broad and flat, and fibrils as narrow and cylindrical[9]. Ribbons will mainly grow by elongation due to LS conditions. As a result of electrostatic interactions, αS monomers in LS repulse each other except for at the ends, which leads to linear growth. Fibrils primarily proliferate by secondary nucleation. If WT monomers are incubated in HS conditions, the repulsive forces between the monomers will lessen due to the charge of ions in the buffer, leading to closer packing and secondary nucleation.

Sometimes a mutation in the amino acid chain can lead to changes in conformation, that eventually result into the formation of a polymorph. Some examples are E46K, where glutamic acid replaced with serine in the 46th place of the chain, and A53T, where alanine is replaced with threonine in the 53th place. Since mutants display different properties from the WT aggregates as well as from themselves, for example higher propensity for form fibrils, these would be worth investigating further.[8]

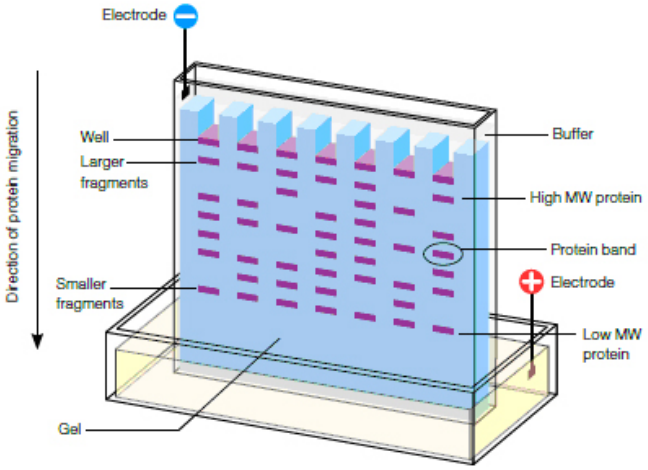

Figure 4 A schematic of SDS-PAGE gel electrophoresis.[15]

2.4 Proteinase K digestion assay

Proteinase K is an enzyme that cleaves serine peptide bonds by hydrolyzing them, fragmenting the protein. These fragments can be visualized through Sodium Docedyl Sulfate-Polyacrlamide Gel Electrophoresis (SDS-PAGE) and staining. An electric field is created with a cathode and anode so that the top of the chamber is negatively charged and the bottom positively. After the samples are pipetted into the wells at the top and travel through the gel, as can be seen in Figure 4, fragments will move through the gel, with speed depending only on size. This is due to the SDS and loading buffer will make the fragments equally negatively charged. Smaller fragments travel faster than the longer fragments, since gels contain pores and smaller fragments can travel easier through those. This results into the shorter and lighter fragments being at the bottom and the longer and heavier fragments at the top. This separation of protein fragments is useful for characterizing proteins and determining whether they are there in a sample. The fragments become visible through staining and will appear as bands. For characterization, a ladder is necessary for comparison. The ladder consists of protein fragments with varying weights. Its function is to make it possible to determine the weight of the bands through comparing the samples and ladder.

There are several characteristics that can be found through a digestion assay. First of all, the time it takes to be fully digested will indicate the number and strength of bonds in each polymorph. Furthermore, band intensity illustrates the number of fragments of the same weight that have been cleaved off. Lastly, the placement of the band represent the molecular weight of the fragment. It is expected to be unique for each polymorph.

2.5 Spectrophotometry

A spectrophotometer makes use of the fluorescent properties of a sample. As can be seen in Figure 5, light passes through a monochromator that lets only a certain range of wavelengths through. Following that, the light travels through a sample, presented in a cuvette, and to the detector. The detector measures the light either transmitted through or absorbed by the sample, depending on the field of interest. As the light source changes in wavelength, so will the intensity. Being able to measure excitation and emission proves helpful in showing to what extent a solvatochromic or fluorogenic dye, more about this in the Section 2.6 has bound to a protein, as well as determining concentrations of substances in a solution.[16]

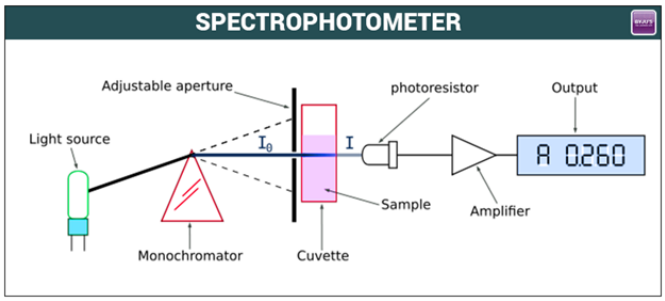

Figure 5 A schematic of an spectrophotometer[16]

2.6 Solvatochromic and Fluorogenic Dyes

Solvatochromic dyes display a shift in excitation and emission, while fluorogenic dyes show a change in fluorescence intensity in response to a change in the environment[17]. Depending on the dye, this change can concern polarity, viscosity or molecular order. Below some examples of these types of dyes will be discussed.

ThT is a dye with an excitation and emission maximum unbound at 385 nm and 445 nm, and bound at 450 and 482 nm respectively, commonly used for staining amyloid fibrils[18]. It is theorized that ThT locks on to grooves of the β-sheet structures, of which the amyloid fibrils have many along the long axis. Due to the extreme increase in intensity caused by rotational immobilization, it is sensitive to rigidity and viscosity and is suited for sensitive detection of amyloids.

Amytracker 630 (Amy) is a dye that binds to beta sheets of aggregates as well. The excitation and emission maxima are respectively 520 nm and 630 nm. Amytracker dyes are Luminescent Conjugated Polythiophenes (LCPs), which are known for binding to protein aggregates. The mechanism is similar to ThT. The intensity of the dye increases once the thiophene backbone locks on to the β-sheets, which makes it suitable for detecting amyloids. Due to this similarity, it is also sensitive to rigidity and viscosity.[19–21]

1-Anilinonaphthalene-8-Sulfonic Acid (ANS) is a dye with excitation and emission peaks of 375 nm and 477 nm respectively[22]. ANS binds through hydrophobic and electrostatic interactions. ANS and amyloids interact through ion pairing between the positively charged amino acids and negatively charged sulfonate groups of the dye. Fluorescence of this dye depends on polarity, viscosity and temperature[23]. In case of amyloids, polarity and viscosity are most important. Since fluorescence increase is activated in apolar, or in other words, hydrophobic environments, formation and quantity of hydrophobic surfaces like β-sheets can be determined through the dye.

Nile Red (NR) increases in terms of fluorescence when activated in hydrophobic environments[24]. Excitation and emission peaks are 559 nm and 635 nm respectively. In polar environments, an electron transfer takes place from the diethylamino group to the aromatic group[23]. This is thermodynamically unfavorable in apolar environments and results into increase in fluorescence, similarly to ANS This makes it useful for detecting β-sheets in amyloids.

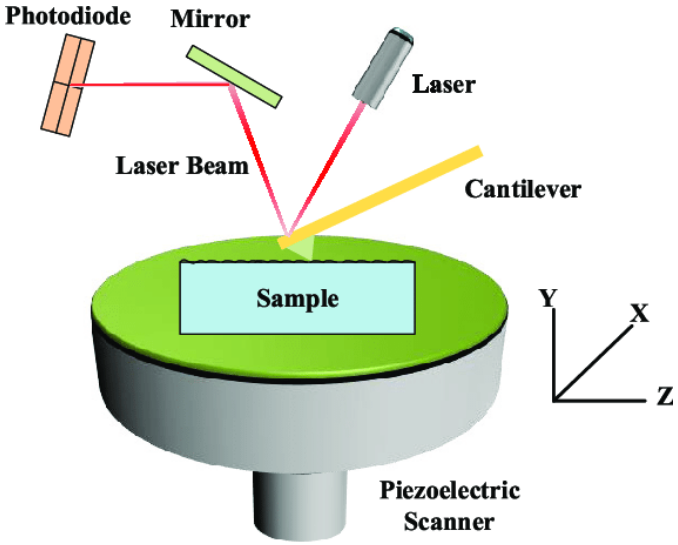

Figure 6 A schematic of an Atomic Force Microscope.[26]

2.7 Atomic Force Microscopy

Atomic Force Microscopy is a technique that scans the topography of a surface of a sample with a tip and cantilever, see Figure 6. The tip taps systematically over the sample. If the tip comes across something, there will be a change in height. As a result, the angle of the laser, that is aimed at the cantilever, would also change. A photodiode will then detect and pass the information to a program to process and create a scan. This technique is used to visualize small structures and in this paper will be used for attempting to characterize different polymorphs.[25]

3 Materials and Methods

3.1 α-Synuclein Fibril Preparation

To obtain different strains for the experiments, monomers aggregated under specific conditions.

A53T and E46K monomers that were in 10 mM Tris-HCl were first aggregated in a shaker (Eppendorf Thermomixer F2.0) for 4 days at 37°C and 1100 rpm. WT αS monomers were put in different solution conditions to develop WT, LS and HS fibrils. WT and LS fibrils were incubated in buffer containing 10 mM Tris-HCl, 10 mM NaCl, 0.3 mM KCl, 1.4 mM CaCl, 1.5 mM $MgCl_2$ and 0.02% w/w NaN_3. For HS fibrils it was

the same with the exception of NaCl being in 15 mM concentration. These concentrations were chosen to imitate cerebrospinal fluid after 10x dilution. WT, E46K and A53T fibrils were sonicated (Branson Sonifier 250) on the intensity setting on 1 for 2 seconds to form seeds. LS and HS fibrils were already in their seeded form, so this process was not necessary for those.

3.2 Seed Amplification Assay

Fibrils stained with ThT were prepared so that aggregation behaviour of strains could be followed over time. Ultimately, lag times of the strains will be compared to see if any can be discriminated from the others. If lag time is not applicable for some condition, then the initial slopes will be determined.

The samples consisted of monomers (20 μM), Thioflavin T (10 μM), NaCl (8.3 mM), buffer (10 mM Tris-HCl, 10 mM KCl) and seeds, where seeds were present in the concentrations 10 nM, 100 nM or 1 μM. The samples were pipetted in a 96-wellsplate (Corning 96-well Half Area Black/Clear Flat Bottom Polystyrene NBS Microplate Cat. No. 3881) in quadruplet, then covered and sealed. In the plate reader (Tecan i-control M200 Pro), the plate was shaken orbitally for 1000 cycles at 37 °C, each cycle consisting of 10 minutes shaking. For the delay time, defined as the time from where every value is twice the plateau value, average (avg) and standard deviation (sd) were calculated for each of the quadruplets, then averaged per condition. For those that did not display a plateau, avg initial slope with sd was calculated instead. Since monomers and dye are added in excess, maximum is expected to reach either there is no more space on the seeds for the dye to bind to.

3.3 Proteinase K Digestion Assay

In this experiment LS, HS and WT fibrils will be digested and put through an SDS-PAGE. The goal is to to compare characteristics like placement of bands, digestion time, band intensity and number of bands of each strain and make out whether they are different from each other.

Fibrils were spun down (Eppendorf Centrifuge 5424R) in 200 μL for 90 minutes at 25 °C. Monomer concentration in LS and HS were determined from the supernatant with the nanodrop (ND-1000 Spectrophotometer) with an extinction coefficient of 5600 $M^{-1}cm^{-1}$ at 276 nm. Next, pellets were taken up in digestion buffer (30 μM Tris-HCl). Monomers and fibrils (40 μM) were incubated at 37°C for exactly 5, 15 and/or 30 minutes with 0.5 (40 μL) proteinase K, after which an equal volume of Tricine SDS sample buffer (Thermo Scientific, LC1676) was added. One of each αS type was kept as a control and thus not incubated with proteinase K. All samples were heated for 5 minutes at 100°C and loaded on a Novex 4-20% Tris-Glycine Plus WedgeWell Gel gel in the Xcell SureLock Mini-Cell using a 1x Tris-Glycine SDS Running Buffer. The ladder (Thermo Scientific™ PageRuler™ Plus Prestained Protein Ladder, 10 to 250 kDa) was also loaded onto the gel. After connecting the chambers to the power supply, the gel was run for 45 minutes at 100 V. After staining the gels with Coomassie Brilliant Blue for 1 hour and destaining for another hour, images were taken with the gel imager (ProteinSimple FluorChem M).

3.4 Photophysical Characterization

Fibrils were stained with a dye and put in a spectrophotometer to determine how well a dye binds to the strain. This will indicate unique structural aspects of different polymorphs in terms of viscosity/rigidity or hydrophobicity depending on the dye. The objective is to find clear shifts in spectra maxima.

Samples were put through the fluorescence spectrophotometer (Varian Eclipse Cary Spectrophotometer) and ran through Cary WinFLR in a cuvette (Hellma Semi-Micro-cuvette 114F-QS, 10x4 mm layer thickness). The excitation and emission spectra were recorded. Seed types include WT, LS, HS, A53T and E46K. The dyes used are ThT, Amy, ANS and NR. Samples contained 600 μL and consisted of seeds (2 μM), their respective monomers (2 μM), dye (200 nM), and buffer, with exception of the conditions concerning LS seeds, HS seeds and ANS dye. Concentrations of seeds and dye were changed to 10 μM for both cases due to otherwise lack of signal. To determine whether monomers have a binding effect with dye, monomer controls were used. Additionally, a dye control was included for each type of dye. As for program settings, scan mode was set to CAT - 2. Detector voltage was set to medium and scan control was put at medium rate. Furthermore, excitation and emission slit were both set to 10 nm. After measurements were taken, spectra were normalized and maxima were determined from these.

3.5 Atomic Force Microscopy

Fibrils were examined using the AFM to determine if strains can be distinguished from each other by their height profile. Eventually height distribution and pitch size of strains will be compared.

Samples were made on mica gels using a concentration of 2 μM for HS, A53T and E46K. These samples were incubated with nitrogen flow for 15 minutes. After that, they were cleaned and dried 3 times using milliQ and left overnight. For the WT sample, the same protocol was followed, but concentration of 1 μM was used with an incubation time of 30 minutes in nitrogen flow. The purpose of this was to let the fibrils set in better, as WT fibrils were difficult to find in previous attempts of this research.

Polymorphs WT, HS, A53T and E46K were characterized by their height as well as the periodicity. As LS and WT fibrils

were stored in the same type of buffer, these should only differ in terms of length, since WT fibrils were sonicated. In terms of morphology, they should be the same. Scans of samples (2 μM) with 10x10 μm format were captured in the Atomic Force Microscope (AFM) (BioScope Catalyst) with Nanoscope (8.15R3sr8) for a general overview. Depending on density, scans of 5x5 μm were taken so that distinct fibrils were visible and could be taken into account for the quantitative analysis. Scans had been made using a scan rate of 0.5 Hz and 512x512 pixels unless stated otherwise. Through NanoScope Analysis 1.5 using the flatten tool, scans were made presentable for height analysis. Fibril height was determined through FiberApp[27]. If the fiber showed clear periodical changes in height through plotting the Height Profile, this fibril was taken into Height Distribution (HD) and Height Discrete Fourier Transform (HDFT) analysis. HD represents in this case the height distribution of all points in the selected fibrils. HDFT is a function that uses the Fourier Transformation to determine the pitch size of objects with periodical height variations such as the selected fibrils. Flatten Order and Smooth Resulting Curve were set to "poly1" and "5" respectively. For the analysis, a minimum of ten fibrils are selected per polymorph.

4 Results and Discussion

4.1 Seed Amplification Assay

The aggregation curves in Appendix A have been used for determining lag time. If lag time was not applicable due to immediate amplification, initial slope was determined instead. This was done as a means to quantify aggregation behaviour, so that strains may be discriminated from each other.

The lag time as well as the initial slope can be found in Figure 7. For all conditions with 1000 nM seeds with the exception of LS, the amplification was immediate and no lag time could be determined. For these the initial slope, where WT shows the lowest initial slope and thus the lowest initial amplification rate, then E46K, then A53T and lastly HS. For 100 nM, the order of amplification rate from slow to fast is the same as for 1000 nM. For the condition 10 nM, this is not the case.

Noticeably, the samples with A53T and E46K seeds show a dramatic increase in lag time compared to the other seeds. For that reason, these fibrils were run for longer. The curves for these can be found in Appendix B. Between the take-out and re-input there is in most conditions a spike visible. This may be due to instrumental reasons. One of the wells of the condition A53T 1 μM seeded shows a decrease. This was due to improper sealing. The other conditions show no significant change. From these results it is suggested 10 nM seeds is too little for these mutants to amplify.

Interestingly, the results show that WT monomers aggregate faster than LS seeds for 100 nM and under. The conditions LS seeded for 10 nM and 100 nM display a longer lag time than the control. This means that the novo fibril formation, which is a process that describes monomers spontaneously aggregating, is dominating the SAA, overshadowing the seed amplification[4].

The mutation A53T amplifying faster than E46K, in other words having a higher propensity for aggregation, is in accordance with a study mentioned in the introduction, although different analysis methods were used[8]. Another study stated A53T and E46K had similar aggregation propensity at a ThT fluorescence assay using a shaking incubator[28]. The first study suggested this difference may be a result of different assembly conditions, for instance the usage of beads in the second study. Furthermore, HS has a higher propensity than LS, which has been shown before too[9,10]. This is a logical development from the difference in main growth mechanism, as secondary nucleation takes place anywhere on the surface of a fibril, and thus has more surface area for the process to take place, while elongation can only happen at the ends, and secondary nucleation takes place more on HS than LS fibrils. Furthermore, it appears the mutants A53T and E46K have a higher propensity than WT, which is in line with previous research[8,29]. It has been hypothesized that for E46K this may be due to Glu residues reducing β-sheet formation in some way. As for A53T it has been stated that the mutation enhances propensity of fibril formation.

Remarkably, the standard deviation of 100 nM WT seeds condition is high due to one outlier. The respective graph in Appendix A also shows it does not align with the other quadruplos. This is likely a result of mispipetting of monomers, as starting intensity was similar to the others.

To sum up, there are significant differences between the strains in lag time and initial slope.

4.2 Proteinase K Digestion Assay

The aim was to differentiate between the various fibril types by comparing the bands of the various strains treated with proteinase K over different incubation periods.

The bands of the ladder were indistinguishable from each other and smudged, see Figure 8. This is due 15 μL of the ladder being loaded on the gel, while 5 μL was the maximum according to the manual[30]. The ladder was overloaded.

Despite proteinase K being expired for 7 years, digestion was successful since volume was adjusted to 0.5 μL to compensate for this. The samples that were not incubated with proteinase K show a few bands. From the non-digested samples, it is already clear that the bands differ from each other. This was also clear in a previous attempt, see Appendix C Figure 22. Digested WT fibrils show a high intensity band in a higher kDa range, while LS does not. HS shows two high intensity bands, one around the same level as WT and another one

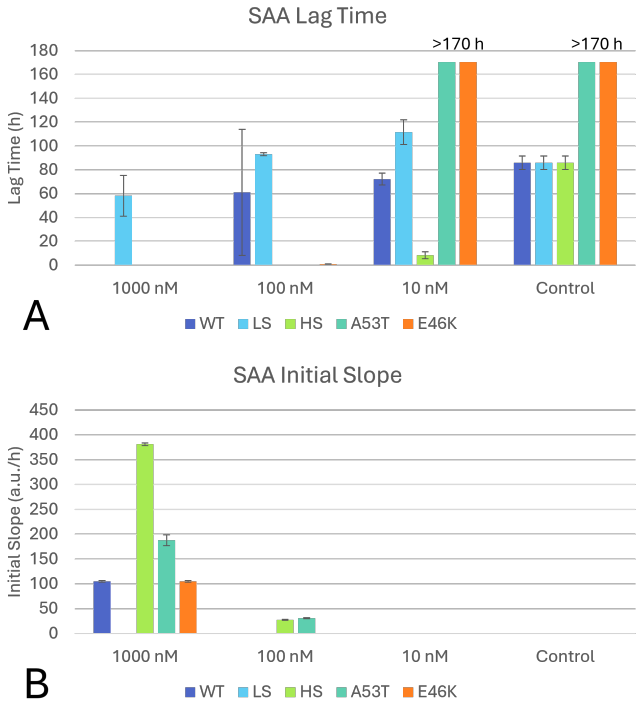

Figure 7 Overview of (A) lag time (h) and (B) initial slope over the conditions with standard deviation. LS and HS conditions contain WT monomers and therefore have the same control as WT seeded. Although conditions A53T and E46K are displayed with a lag time of 170 hours, they have a lag time of over 1965 cycles (335 hours) for 10 nM seed concentration and controls.

lower, although it is possible that the fragments from HS will travel further into the gel, resulting into multiple less intense bands.

Curiously, the separation range is 8-250 kDa according to the product manual, but according to the product site it is 20-200 kDa for this type of gel. Previous research has shown that the digested bands should be found in less than 15 kDa, and as the bands were not separated, it must be that the true separation range was 20-200 kDa[10,31]. Thus, the digested fibrils are expected to be "further down the gel" at a lower weight level. In other words, another type of gel should be used.

Noticeably, the conditions LS 15 and HS 30 display a lower band intensity. This is likely due to mispipetting, as the previous experiment in Appendix C Figure 22 did now show this.

In short, it has been gathered from this that the experiment should be redone with the right materials to be able to draw a conclusion.

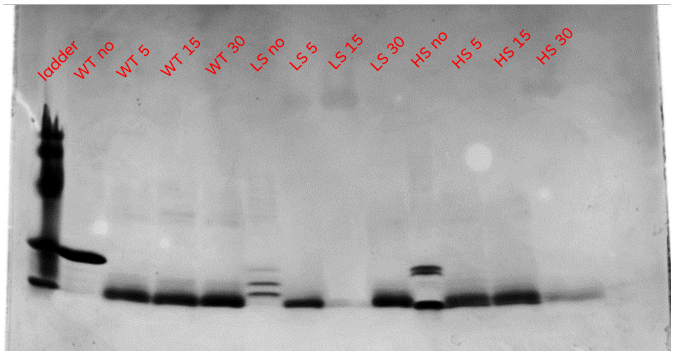

Figure 8 Image of gel that shows the bands of undigested as well as digested fibrils and the ladder. Conditions are stated in red, with polymorph type first and incubation time with proteinase K after.

4.3 Photophysical Characterization

Difference between wavelength respective to maxima and wavelength respective to dye control were determined for each strain. Shifts and intensities were compared to find out whether strains can be discriminated in terms of rigidity and hydrophobicity.

Spectra are shown in Figures 9 and 10. Some shifts in spectra are clearly visible already, as can be seen in Figure 11. Spectra of the controls can be found in Appendix D. It is shown that monomers do not affect the spectra. Spectra without normalization can be found in Appendix E.

For **ThT** in terms of excitation, LS shifts to unbound dye more than other strains. HS fibrils display a higher intensity in both excitation and emission spectra, see Appendix E 25 (A) and (B). LS fibrils show an intensity on the low side, although the difference in intensity is not as dramatic as with HS. According to literature β-sheet content of WT, E46K and A53T are 68%, 66% and 68% respectively[29]. As for ribbons and fibrils, the content should be 79.5% and 75.2%. Despite that, fibrils (HS) were found to bind ten times better than ribbons (LS) to ThT in the same concentration, which is in line with the results[9]. It appears that ThT binding depends on morphology rather than β-sheet content[29].

Furthermore, for **Amy** A53T stands out in terms of excitation and HS in terms of emission. A53T has an excitation peak maximum that is not similarly high or low to other strains. Interestingly, LS is hard to distinguish from the other strains in terms of excitation shift, unlike when it binds ThT.

Next, for **ANS** LS in terms of emission and HS in terms of excitation and emission stand out. ANS binds to hydrophobic surfaces. From Figure 24 in Appendix E it appears that the excitation and emission peak of unbound ANS is 345 nm and 525 nm. Compared to the other polymorphs, HS shows a bigger shift towards bound dye, while LS shows that for unbound dye.

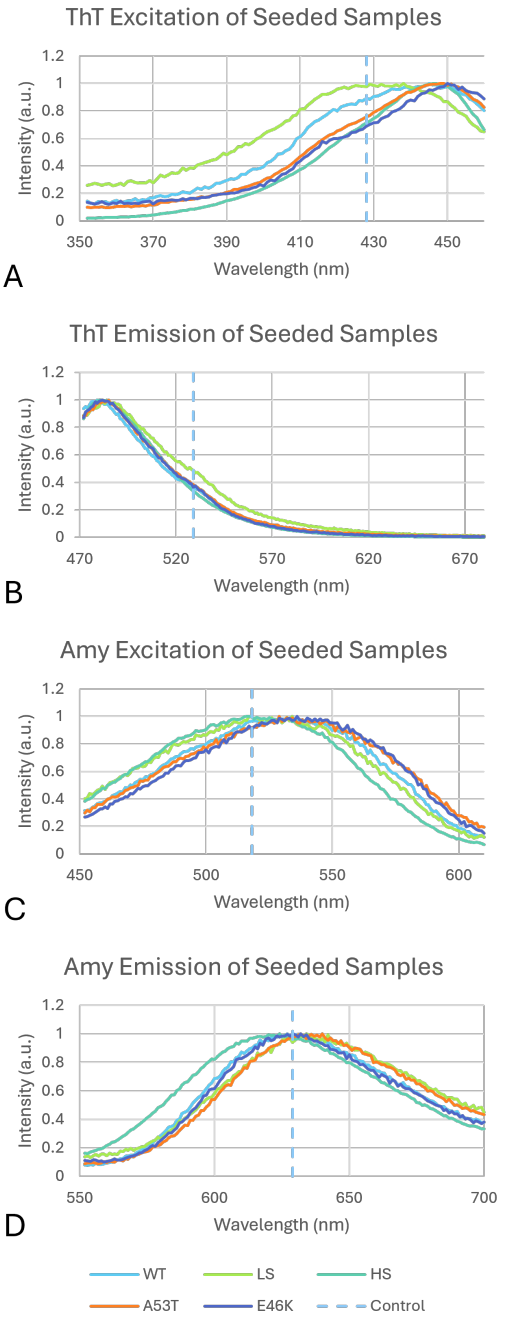

Figure 9 Excitation and emission spectra of the polymorphs for the dyes ThT and Amy. The legend displays which colour represents which polymorph. The vertical line named control stands for the position of the maximum that was measured in control that contained dye and buffer only.

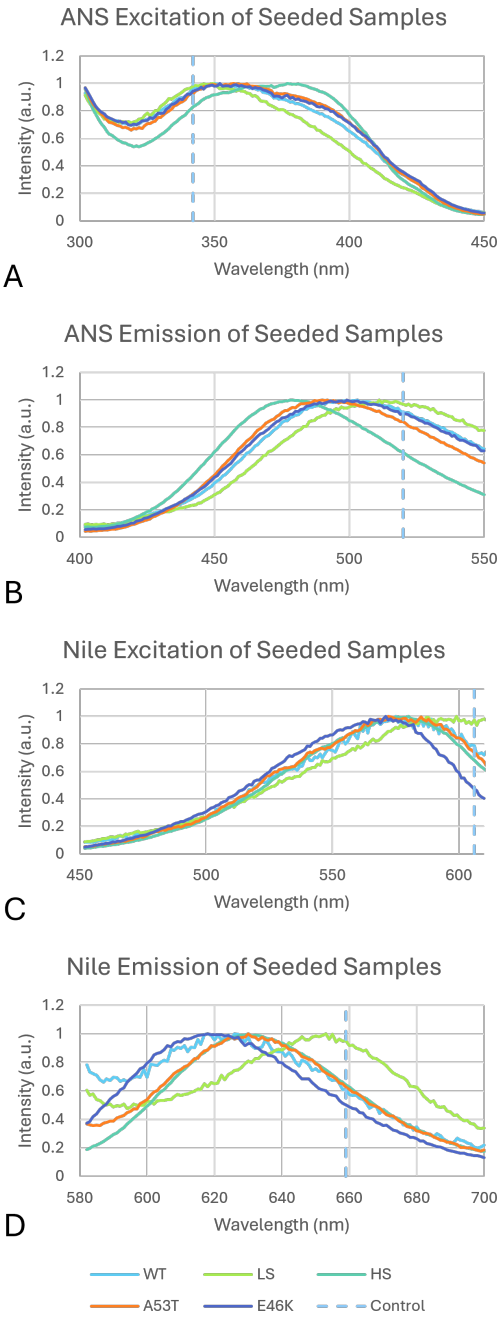

Figure 10 Excitation and emission spectra of the polymorphs for the dyes ANS and NR. The legend displays which colour represents which polymorph. The vertical line named control stands for the position of the maximum that was measured in control that contained dye and buffer only.

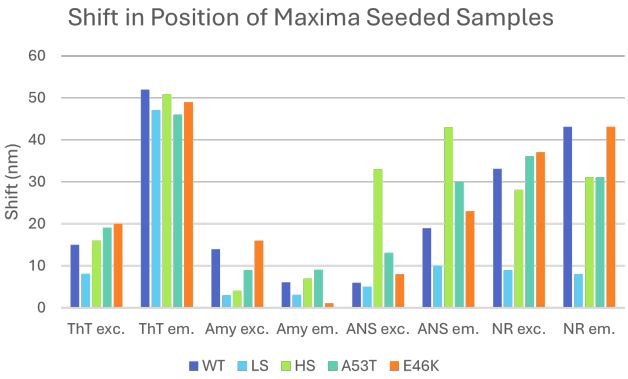

Figure 11 Shift in position of maxima compared to dye control grouped by dye and excitation/emission of seeded samples.

It appears that HS is hydrophobic, while LS is hydrophilic, relatively speaking. This can also be seen in terms of intensity in Appendix A Figure 27 (A) and (B).

Lastly, for **NR** LS in terms of excitation as well as emission stand out and HS in terms of excitation. Unbound NR has an excitation and emission peak at 600 and 655 nm and bound dye 559 nm and 635 nm respectively. LS shifts towards higher wavelengths. It is shown that LS fibrils are more hydrophilic than other polymorphs control show that. HS fibrils, on the other hand, do not bind as well to the dye as with ANS. This may be due to that ANS also binds through electrostatic interactions.

As the spectra of the monomer controls and dye control are alike, it can be concluded that monomers do not interact with the dyes, see Appendix F.

All in all, some strains can be uniquely defined by their spectra depending on the dye.

4.4 Atomic Force Microscopy

Scans of fibril topography were taken. From these, height distribution and periodicity were determined with Fiberapp. These properties will be compared to find out if one can discriminate strains based on these.

As can be seen in Figure 12, the HS and E46K fibrils were found in high density and thus were unpractical for data analysis, which is why zoomed in scans of these polymorphs were made, see Figure 13. Using subfigures (A) and (C) from Figure 12 and (A) and (B) from Figure 13, height distribution and periodicty were found, see Figures 14 and 15 respectively.

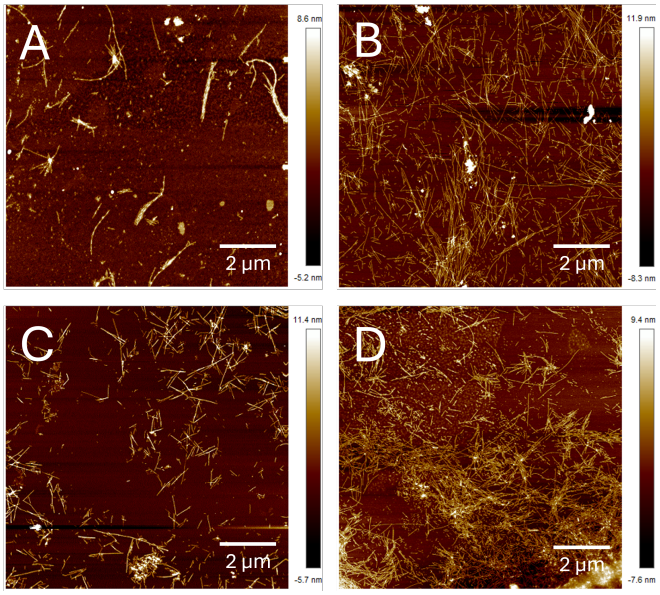

Figure 12 An overview of the scans made with the AFM. Fibrils shown are in following order: (A) WT, (B) HS, (C) A53T, (D) E46K. The size of the scans are 10x10μm. Subfigure (A) was captured using 1024 lines instead of 512, due to little fibrils being present on the sample. To increase the number of fibrils that display a clear periodical changes in height for analysis, quality of scan was increased by doubling the number of lines.

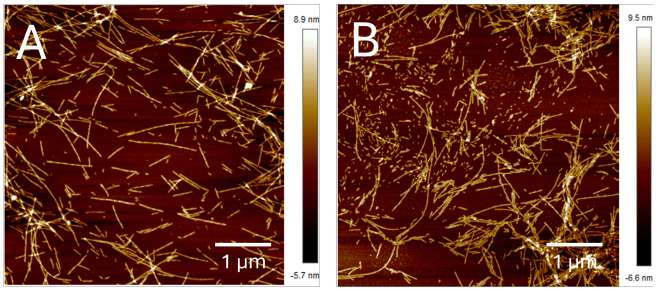

Figure 13 An overview of the zoomed in scans made with the AFM due to high density. Fibrils are (A) HS and (B) E46K. The size of the scans are 5x5μm.

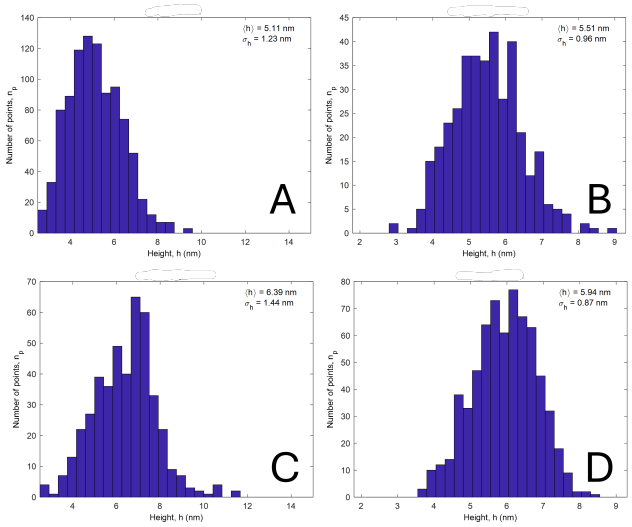

Figure 14 An overview of the height distributions. Polymorphs are shown in following order: (A) WT, (B) HS, (C) A53T, (D) E46K.

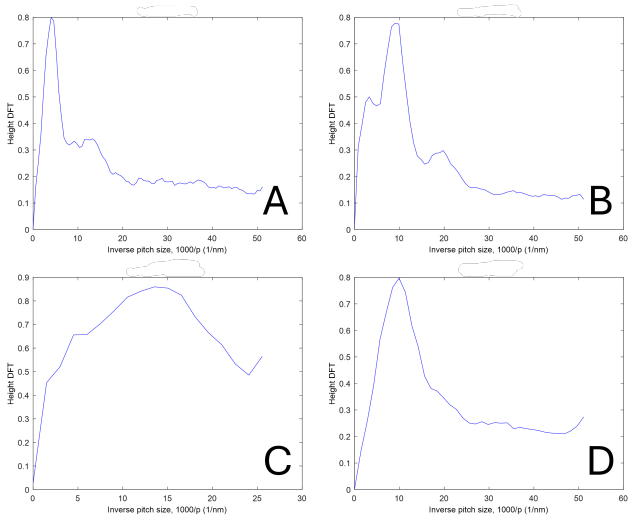

Figure 15 An overview of the discrete Fourier transformations applied to the height of the fibers. Polymorphs are in following order: (A) WT, (B) HS, (C) A53T and (D) E46K.

In all subfigures a normal distribution can be seen. Average height (avg) $\pm$ standard deviation (sd), inverse pitch size and respective pitch size can be found in Table 1. A53T displays the largest height, then E45K, after that HS fibrils and lastly WT fibrils. Both the avg and sd are estimated by Fiberapp. The sd is high enough for each polymorph high, leading to overlap between them. The avg is lower than expected[29]. This could be a due to using a different buffer or incubation method. The overlap in height is around the same proportion as found before.

Interestingly, WT and HS display more than one peak, showing that the periodicities of these polymorphs tend to diverge to more than one value. As these fibril fragment lengths tend to have more than one value, they are considered heterogeneous fibrils. This is in accordance with literature for WT αS[29]. WT fibrils illustrate another peak at 12.64 nm, which equals to a periodicity of 79.09 nm. Other values for HS include 2.23 nm and 19.95 nm, which converts to a periodicity of 448.53 nm and 50.12 nm respectively.

Furthermore, measurements of A53T display a relatively broad peak, suggesting the periodicity of this polymorph gravitates less to a certain value. The average periodicity is lower than expected and should be around 300 nm[29]. This could be a result of taking many heterogeneous fibrils that were on the shorter side.

To summarize, the periodicities differ significantly and each of them can be distinguished from each other. For height distribution, however, this is not the case.

Polymorph	Height avg. $\pm$ sd (nm)	Max inv. pitch (1000/nm)	Periodicity (nm)
WT	5.11 ± 1.23	4.02	248.57
HS	5.51 ± 0.96	9.07	110.30
A53T	6.39 ± 1.44	13.53	73.93
E46K	5.94 ± 0.87	9.94	100.64

Table 1 Average height and standard deviation of each polymorph derived from the AFM images.

4.5 Conclusion and Future Perspectives

The goal of this research was to find a way to characterize and distinguish the strains WT, LS, HS, A53T and E46K.

It has been concluded that it is possible to differentiate strains by SAA through lag time and initial slope if seed concentration is high enough. If seed concentration is below 10 nM, mutants A53T and E46K will not aggregate for at least 335 hours. As for the digestion assay, no conclusion could be drawn with current results. Furthermore, it has been shown that through measuring fluorescence of the dyes ThT, Amy, ANS and NR, bound to the strains, only polymorphs LS, HS and A53T could be discriminated from the others. Lastly, from the results of the AFM analysis, it can be concluded that from height distribution the strains cannot be discriminated from each other, but from periodicity, that is possible.

This research focused on distinguishing a few selected strains. For further studies, it is important to find a relationship on how the strains affect synucleinopathies. Once SAA is available on the market and SAA results can be connected to synucleinopathy, care path can be specified and quality of life can be improved. Moreover, different characteristics can be analyzed with the same method, for instance the time it takes for fluorescence to reach the maximum in an SAA. Experiments can also be extended by using other dyes for spectrophotometry, like Congo Red, and researching strain characteristics over time with the AFM or spectrophotometer. Additionally, it could be of interest to investigate with more techniques that describe other characteristics, for example Circular Dichroism (CD) Spectroscopy, Fourier Transform Infrared (FTIR), spectroscopy and in vitro analysis. Lastly, future research for differentiating polymorphs should generally include other αS types to analyze.

References

[1] Mhyre TR, Boyd JT, Hamill RW, Maguire-Zeiss KA. Parkinson's Disease. 2012 Sub-cellular biochemistry; 65:389. doi:10.1007/978-94-007-5416-4_16.

[2] Cleveland Clinic. Parkinson's Disease: What It Is, Causes, Symptoms & Treatment ; 2022.

[3] Chen R, Gu X, Wang X. α-Synuclein in Parkinson's disease and advances in detection. 2022 Clinica Chimica Acta; 529:76-86. doi:10.1016/J.CCA.2022.02.006.

[4] Vaneyck J, Yousif TA, Segers-Nolten I, Blum C, Claessens MMAE. Quantitative Seed Amplification Assay: A Proof-of-Principle Study. 2023 Journal of Physical Chemistry B; 127(8):1735-43. doi:https://doi.org/10.1021/acs.jpcb.2c08326.

[5] Siderowf A, Concha-Marambio L, Lafontant DE, Farris CM, Ma Y, Urenia PA, et al. Assessment of heterogeneity among participants in the Parkinson's Progression Markers Initiative cohort using α-synuclein seed amplification: a cross-sectional study. 2023 The Lancet Neurology; 22(5):407. doi:10.1016/S1474-4422(23)00109-6.

[6] Smith L, Schapira AHV. GBA Variants and Parkinson Disease: Mechanisms and Treatments. 2022 Cells; 11(8). doi:10.3390/CELLS11081261.

[7] Schmidt S, Stautner C, Vu DT, Heinz A, Regensburger M, Karayel O, et al. A reversible state of hypometabolism in a human cellular model of sporadic Parkinson's disease. 2023 Nature Communications 2023 14:1; 14(1):1-24. doi:10.1038/s41467-023-42862-7.

[8] Greenbaum EA, Graves CL, Mishizen-Eberz AJ, Lupoli MA, Lynch DR, Englander SW, et al. The E46K Mutation in α-Synuclein Increases Amyloid Fibril Formation. 2005 Journal of Biological Chemistry; 280(9):7800-7. doi:10.1074/JBC.M411638200.

[9] Bousset L, Pieri L, Ruiz-Arlandis G, Gath J, Jensen PH, Habenstein B, et al. Structural and functional characterization of two alpha-synuclein strains. 2013 Nature communications; 4. doi:10.1038/NCOMMS3575.

[10] Lau D, Tang Y, Kenche V, Copie T, Kempe D, Jary E, et al. Single molecule fingerprinting reveals different growth mechanisms in seed amplification assays for different polymorphs of αSynuclein fibrils. 2024 bioRxiv :2024.03.05.583619. doi:10.1101/2024.03.05.583619.

[11] Sakunthala A, Datta D, Navalkar A, Gadhe L, Kadu P, Patel K, et al. Size-dependent secondary nucleation and amplification of α-synuclein amyloid fibrils. 2021 bioRxiv :2021.12.28.474324. doi:10.1101/2021.12.28.474324.

[12] Mehra S, Gadhe L, Bera R, Sawner AS, Maji SK. 2021 biomolecules Structural and Functional Insights into α-Synuclein Fibril Polymorphism. doi:10.3390/biom11101419.

[13] Slope - Wikipedia ;.

[14] McCann H, Stevens CH, Cartwright H, Halliday GM. α-Synucleinopathy phenotypes. 2014 Parkinsonism & Related Disorders; 20(SUPPL.1):S62-7. doi:10.1016/S1353-8020(13)70017-8.

[15] SDS-PAGE - Kenzo ;.

[16] Principle of Spectrophotometer and its Applications— Chemistry— Byjus ;.

[17] Klymchenko AS. Solvatochromic and Fluorogenic Dyes as Environment-Sensitive Probes: Design and Biological Applications. 2017 Accounts of Chemical Research; 50(2):366-75. doi:10.1021/ACS.ACCOUNTS.6B00517/ASSET/IMAGES/MEDIUM/AR-2016-005173_0011.GIF.

[18] Biancalana M, Koide S. Molecular Mechanism of Thioflavin-T Binding to Amyloid Fibrils. 2010 Biochimica et biophysica acta; 1804(7):1405. doi:10.1016/J.BBAPAP.2010.04.001.

[19] Amytracker 630 – Ebba Biotech AB ;.

[20] Pretorius E, Page MJ, Hendricks L, Nkosi NB, Benson SR, Kell DB. Both lipopolysaccharide and lipoteichoic acids potently induce anomalous fibrin amyloid formation: assessment with novel Amytracker™ stains. 2018 Journal of the Royal Society Interface; 15(139). doi:10.1098/RSIF.2017.0941.

[21] Åslund A, Sigurdson CJ, Klingstedt T, Grathwohl S, Bolmont T, Dickstein DL, et al. Novel pentameric thiophene derivatives for in vitro and in vivo optical imaging of a plethora of protein aggregates in cerebral amyloidoses. 2009 ACS Chemical Biology; 4(8):673-84. doi:10.1021/CB900112V/SUPPL_FILE/CB900112V_SI_002.AVI.

[22] Spectrum [1,8-ANS] — AAT Bioquest ;.

[23] Hawe A, Sutter M, Jiskoot W. Extrinsic Fluorescent Dyes as Tools for Protein Characterization. 2008 Pharmaceutical Research; 25(7):1487. doi:10.1007/S11095-007-9516-9.

[24] Nile Red *CAS 7385-67-3* — AAT Bioquest ;.

[25] Ishida N. Atomic force microscopy. 2023 Non-Destructive Material Characterization Methods :89-125. doi:10.1016/B978-0-323-91150-4.00011-2.

[26] Illustration of atomic force microscope. — Download Scientific Diagram ;.

[27] Usov I, Mezzenga R. FiberApp: An open-source software for tracking and analyzing polymers, filaments, biomacromolecules, and fibrous objects. 2015 Macromolecules; 48(5):1269-80. doi:10.1021/MA502264C/ASSET/IMAGES/LARGE/MA-2014-02264C_0012.JPEG.

[28] Choi W, Zibaee S, Jakes R, Serpell LC, Davletov B, Anthony Crowther R, et al. Mutation E46K increases phospholipid binding and assembly into filaments of human α-synuclein. 2004 FEBS Letters; 576(3):363-8. doi:10.1016/J.FEBSLET.2004.09.038.

[29] Sidhu A. 2016 Multifaceted fibrils: self-assembly, polymorphism and functionalization. doi:10.3990/1.9789036540247.

[30] Thermo Scientific™ PageRuler™ Plus Prestained Protein Ladder, 10 to 250 kDa 10 x 250μL — Fisher Scientific ;.

[31] Novex™ Tris-Glycine Mini Protein Gels, 4–20%, 1.0 mm, WedgeWell™ format ;.

[32] Roche. Great information-compact format-the RAS Lab FAQS, 3 rd edition.

5 Appendices

5.1 Appendix A: SAA Curves

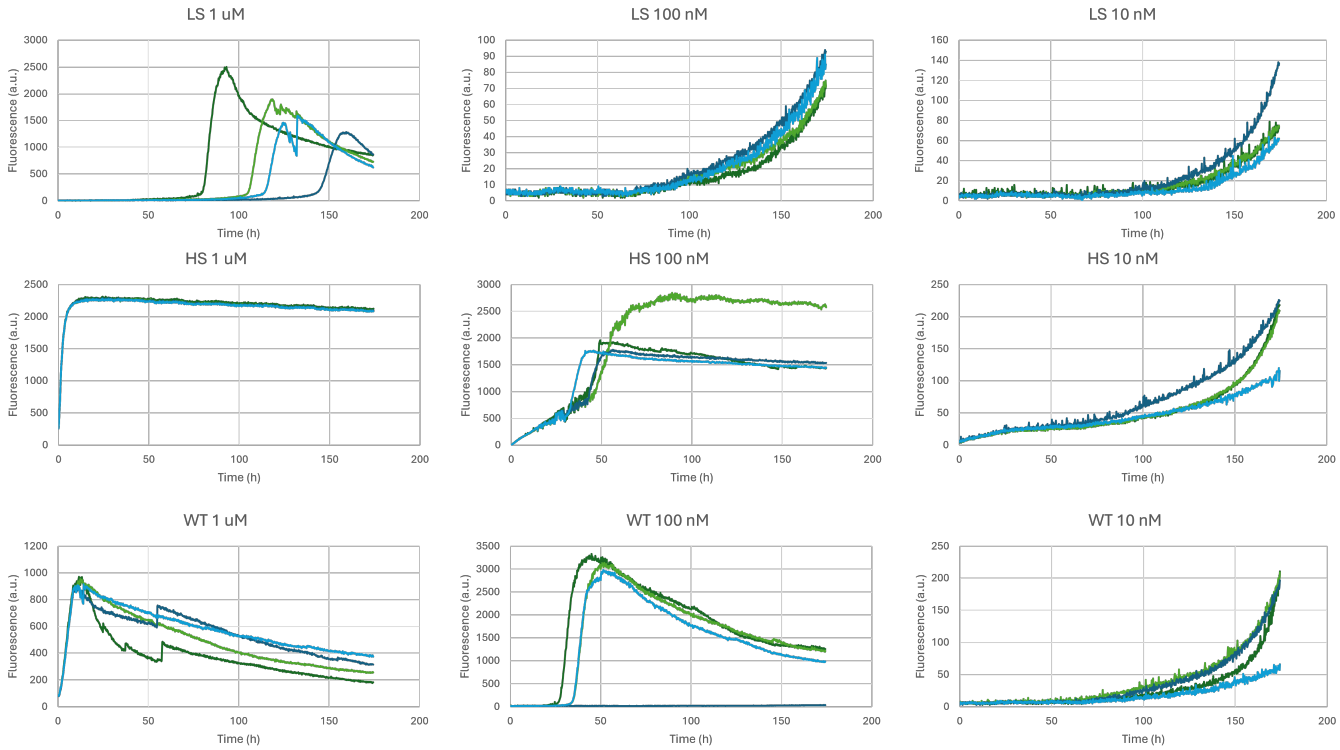

Figure 16 Overview of SAA graphics of polymorphs LS, HS and WT in concentrations 1 μM, 100 nM and 10 nM.

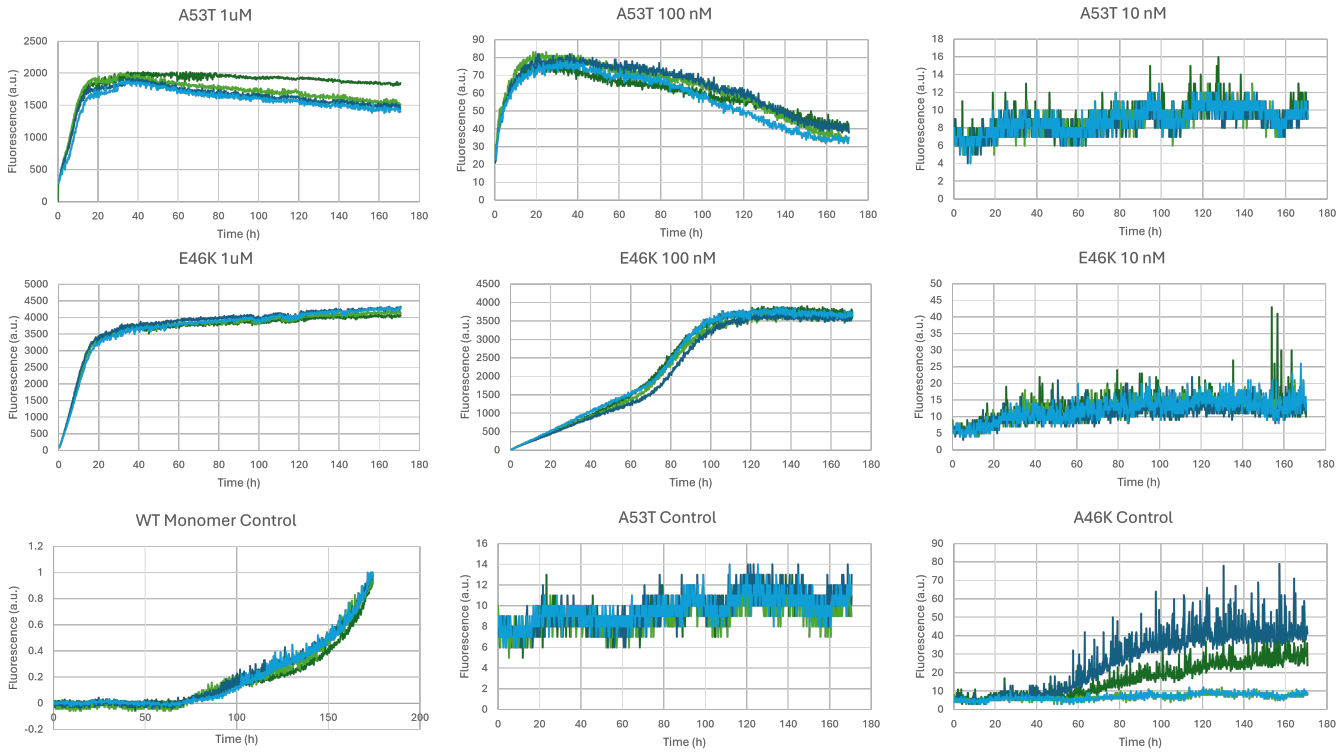

Figure 17 Overview of SAA graphics of polymorphs A53T and E46K in concentrations 1 μM, 100 nM and 10 nM, as well as the monomer controls.

5.2 Appendix B: SAA 335 Hours Mutants

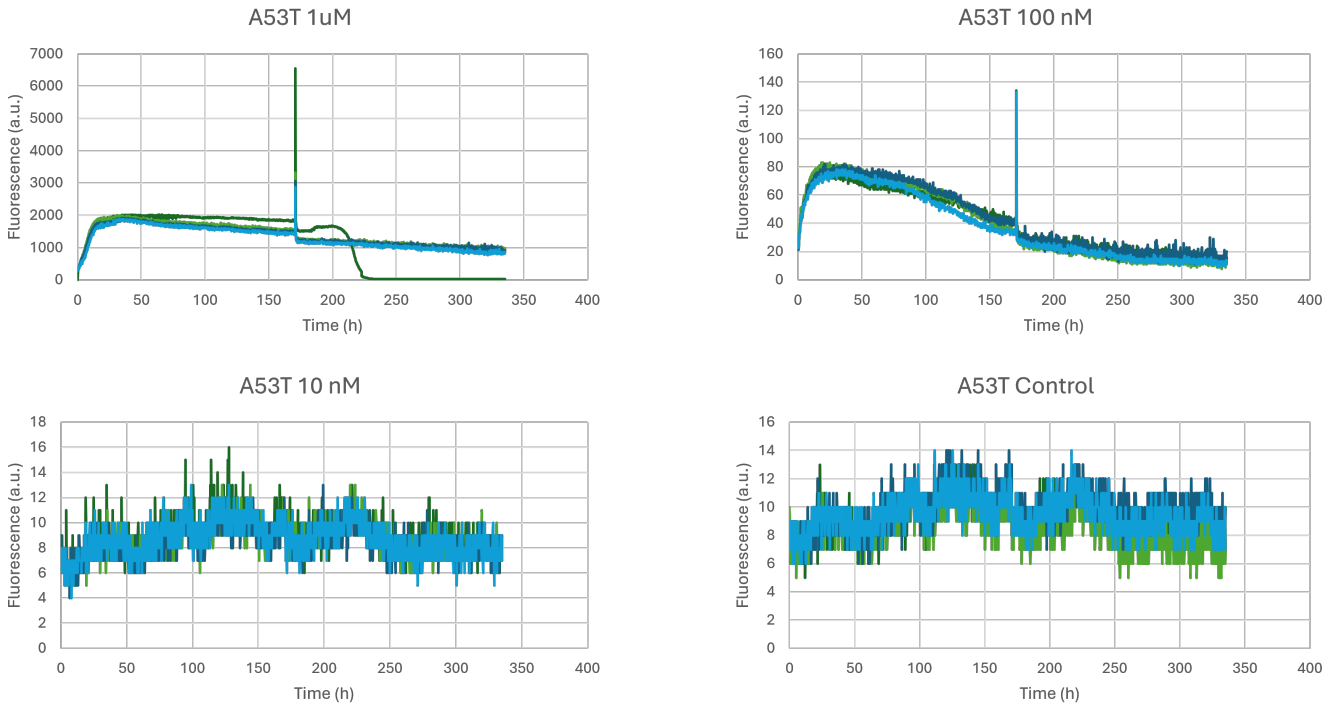

Figure 18 Overview of SAA graphics of A53T in concentrations 1 μM, 100 nM and 10 nM over the duration of 335 hours.

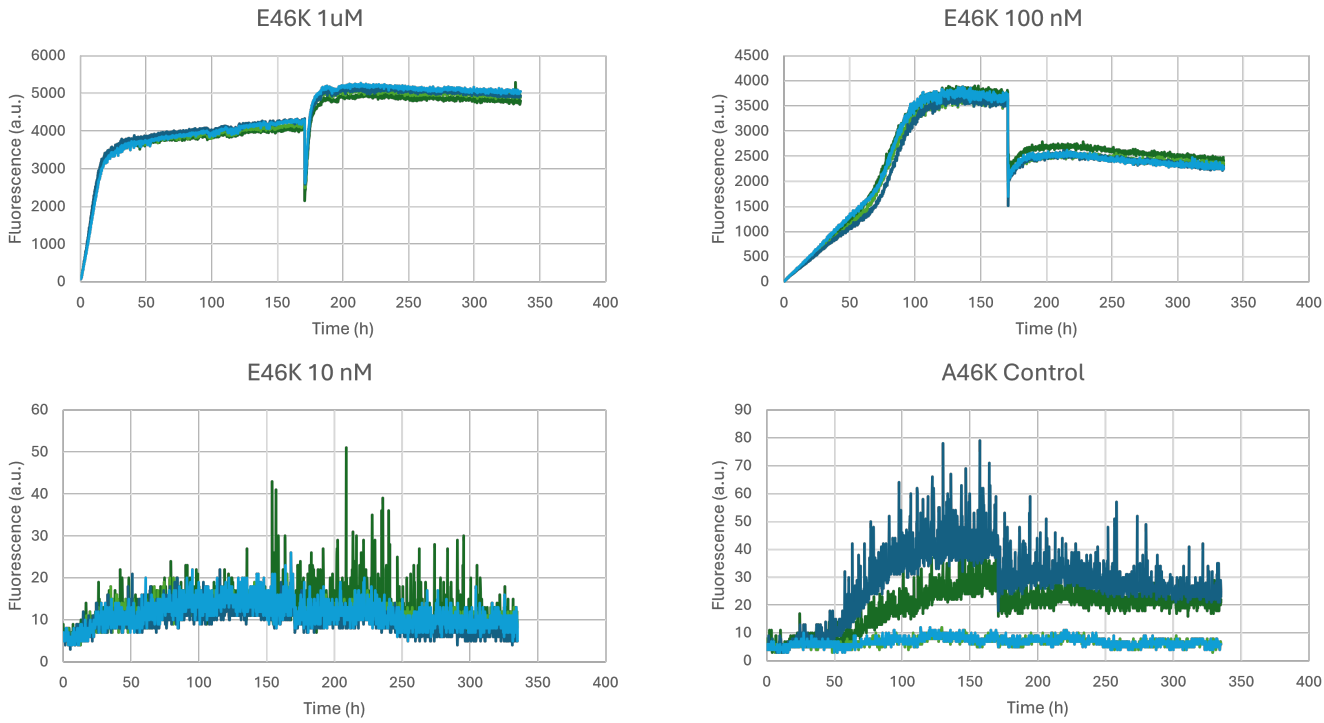

Figure 19 Overview of SAA graphics of E46K in concentrations 1 μM, 100 nM and 10 nM over the duration of 335 hours.

5.3 Appendix C: Previous Attempts at Proteinase K Digestion Assay

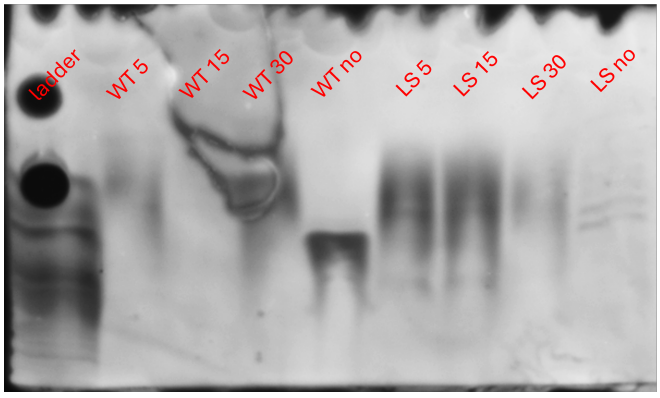

Figure 20 Image of the first gel that shows the bands of undigested as well as digested fibrils and the ladder. Conditions are stated in red, with polymorph type first and incubation time with proteinase K after. Samples were loaded on a 8-16% mini-protean TGX gel in the Bio-rad mini-protean system using a cathode and anode buffer. It was first ran on 30 V for 1 hour, then 150 V for 4 to 5 hours[32]. Buffer was made with 1 M Tris and 0.1 M Tricine, which makes the bands appear faded.. This was an unplanned deviation from the protocol.

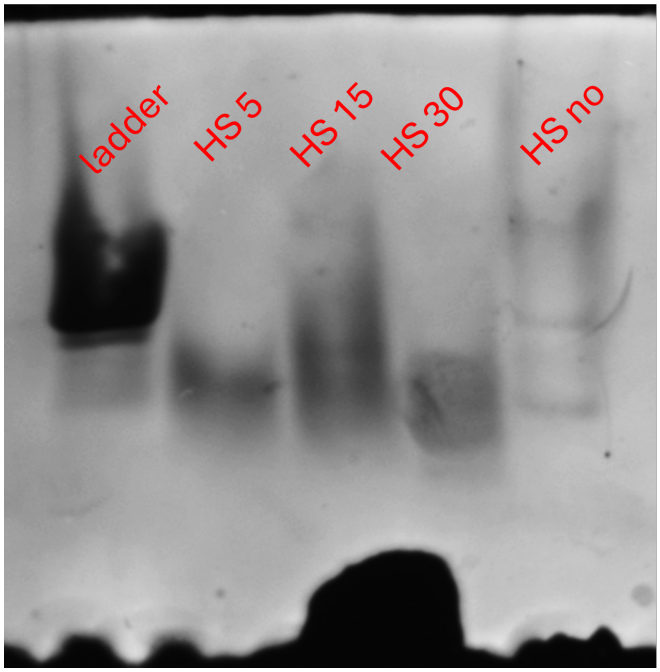

Figure 21 Image of the second gel corresponding to Figure 20 that shows the bands of undigested as well as digested fibrils and the ladder. Conditions are stated in red, with polymorph type first and incubation time with proteinase K after.

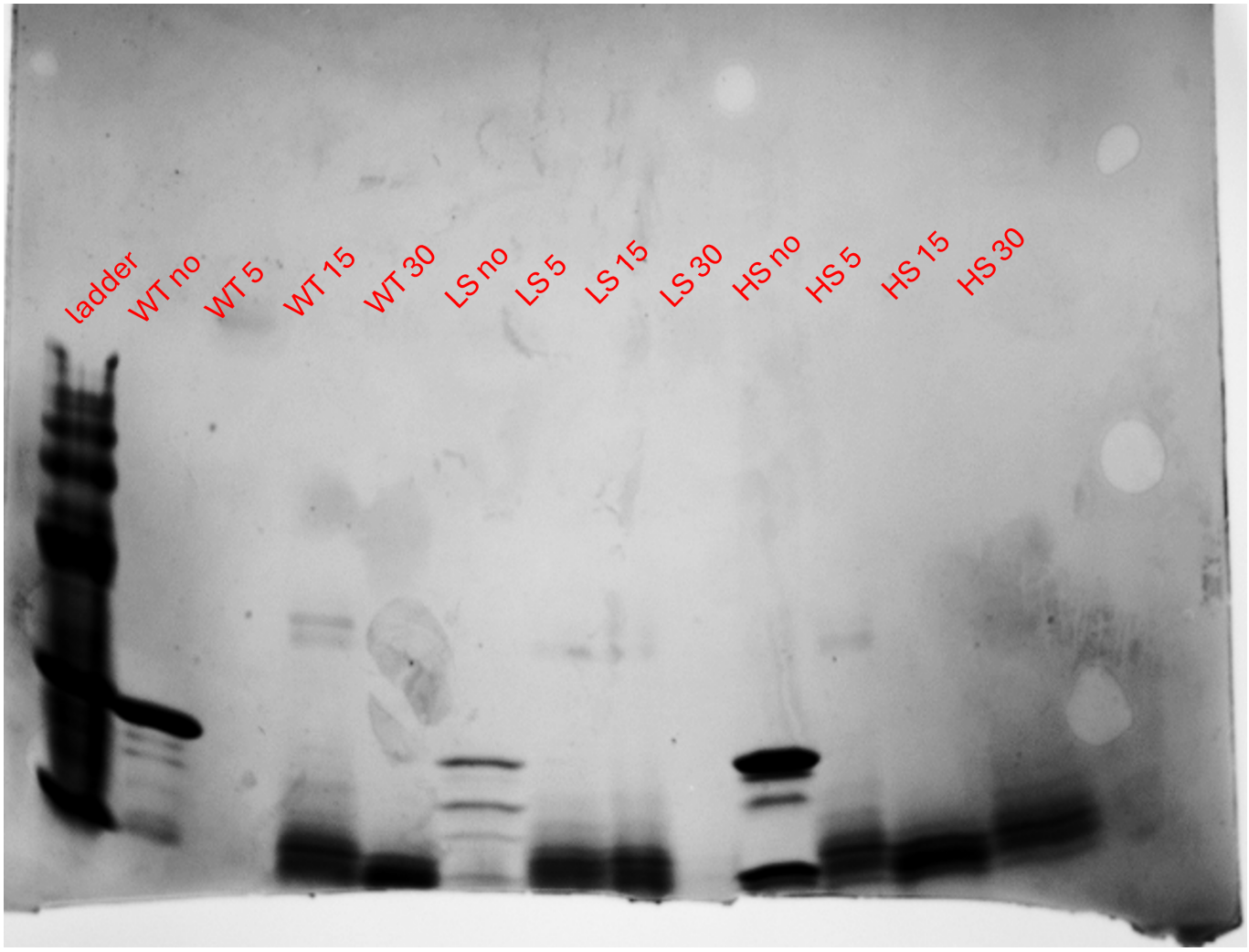

Figure 22 Image of gel that shows the bands of undigested as well as digested fibrils and the ladder. Conditions are stated in red, with polymorph type first and incubation time with proteinase K after. This gel was run on 225V for 30 minutes

5.4 Appendix D: Spectra of Controls

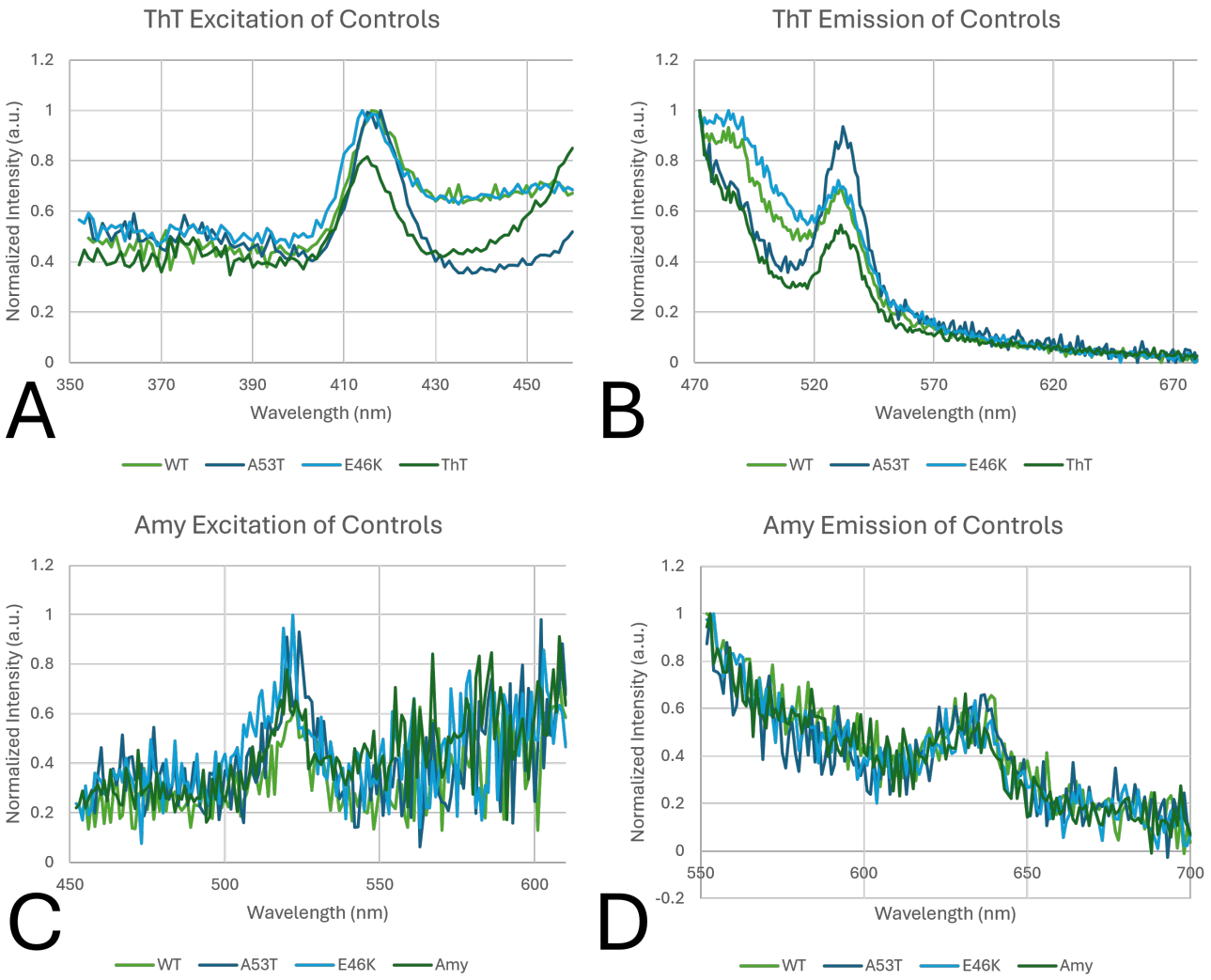

Figure 23 Overview of spectra from controls that contained no seeds. the excitation and emission spectra that are displayed are of ThT and Amy.

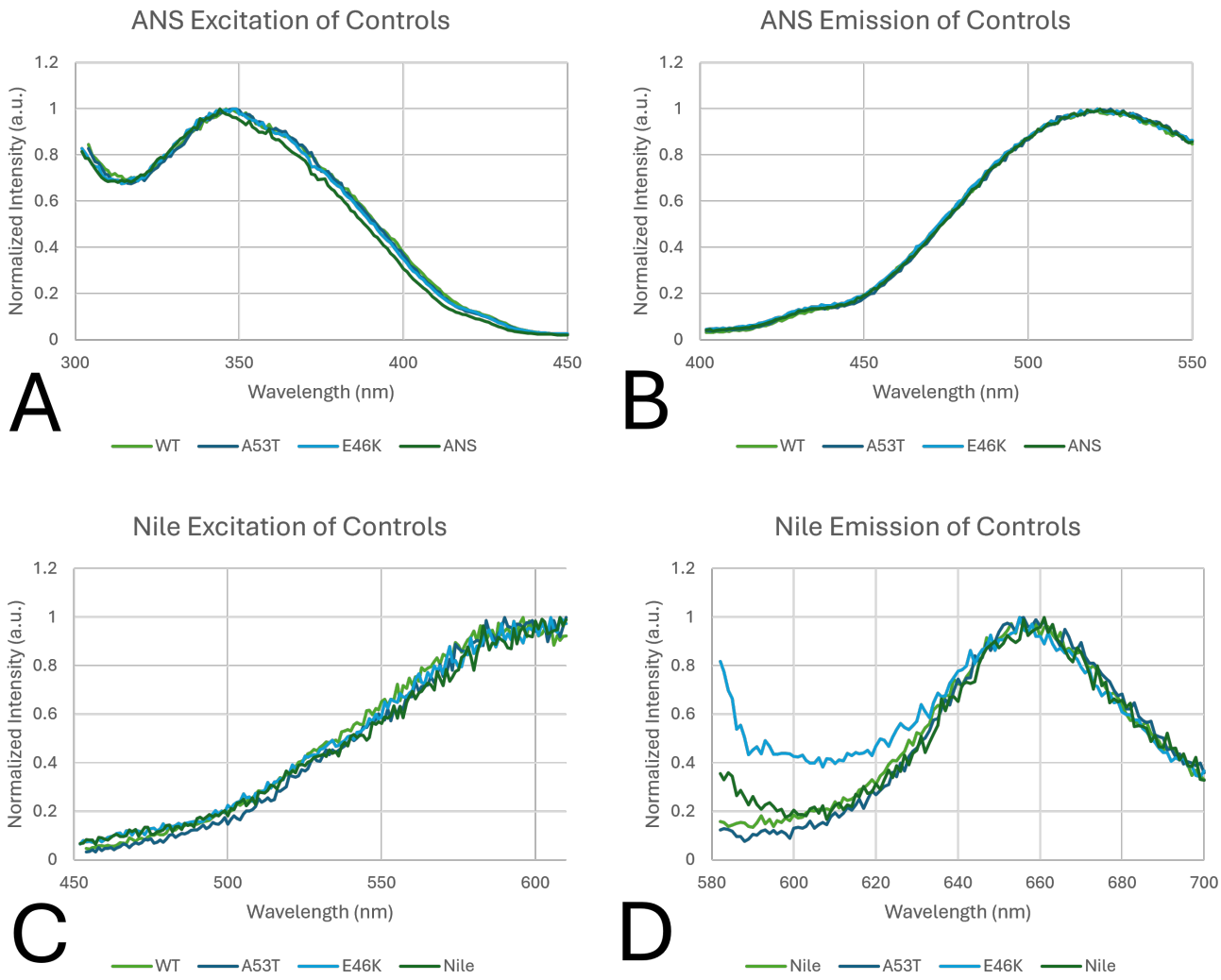

Figure 24 Overview of spectra from controls that contained no seeds. the excitation and emission spectra that are displayed are of ANS and NR.

5.5 Appendix E: Spectra Without Normalization

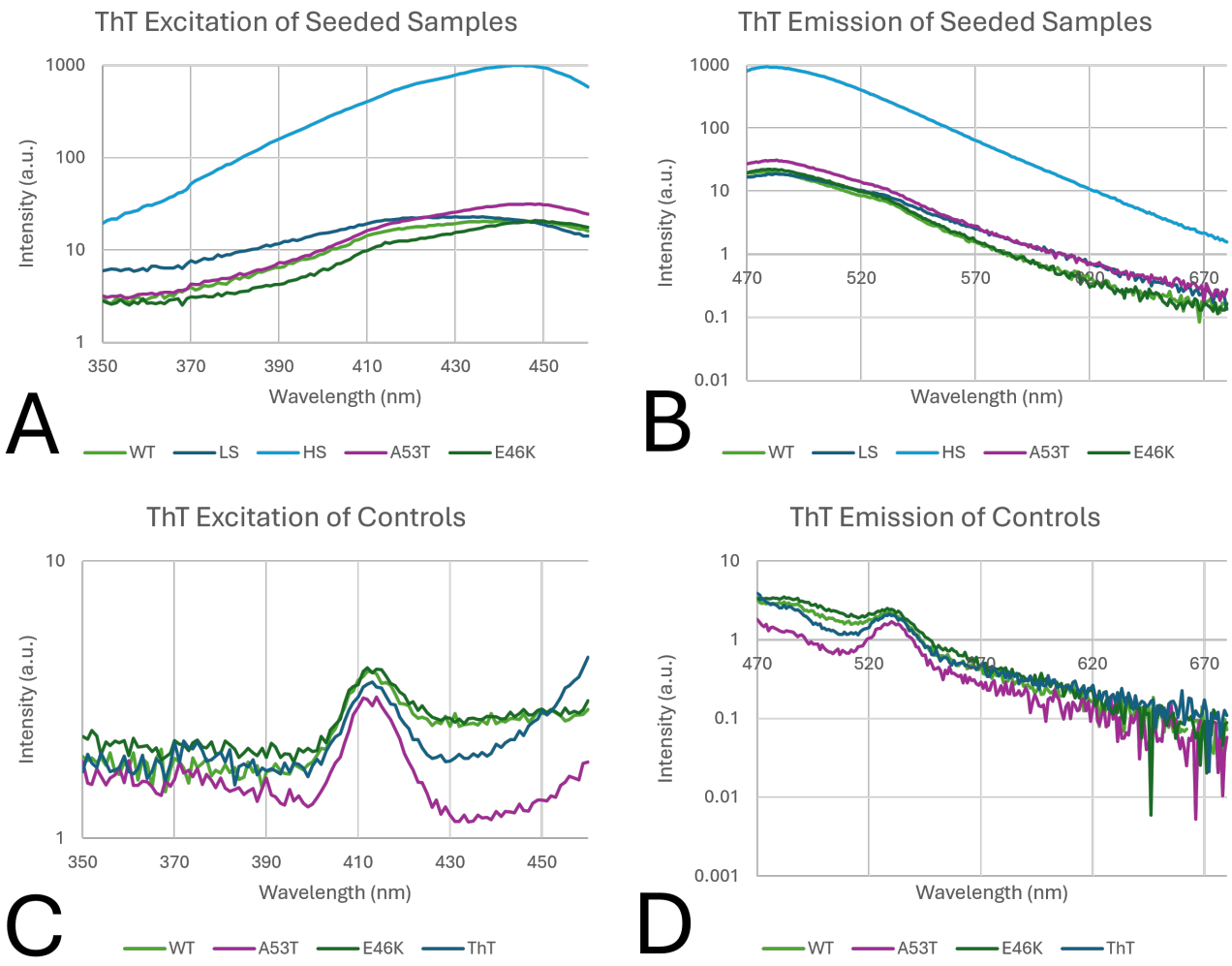

Figure 25 Excitation and emission spectra of seeded samples as well as controls dyed with ThT with log scale.

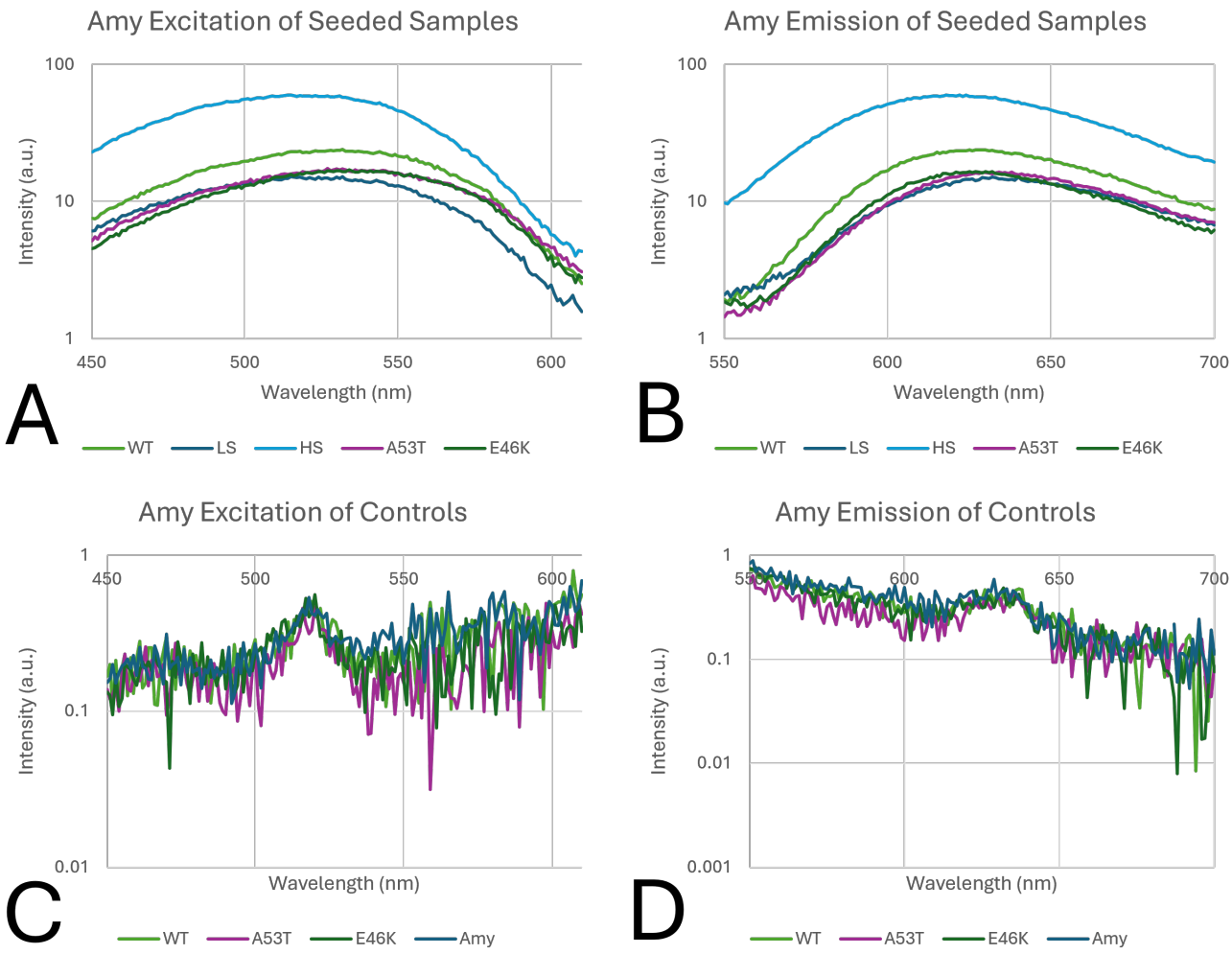

Figure 26 Excitation and emission spectra of seeded samples as well as controls dyed with Amy with log scale.

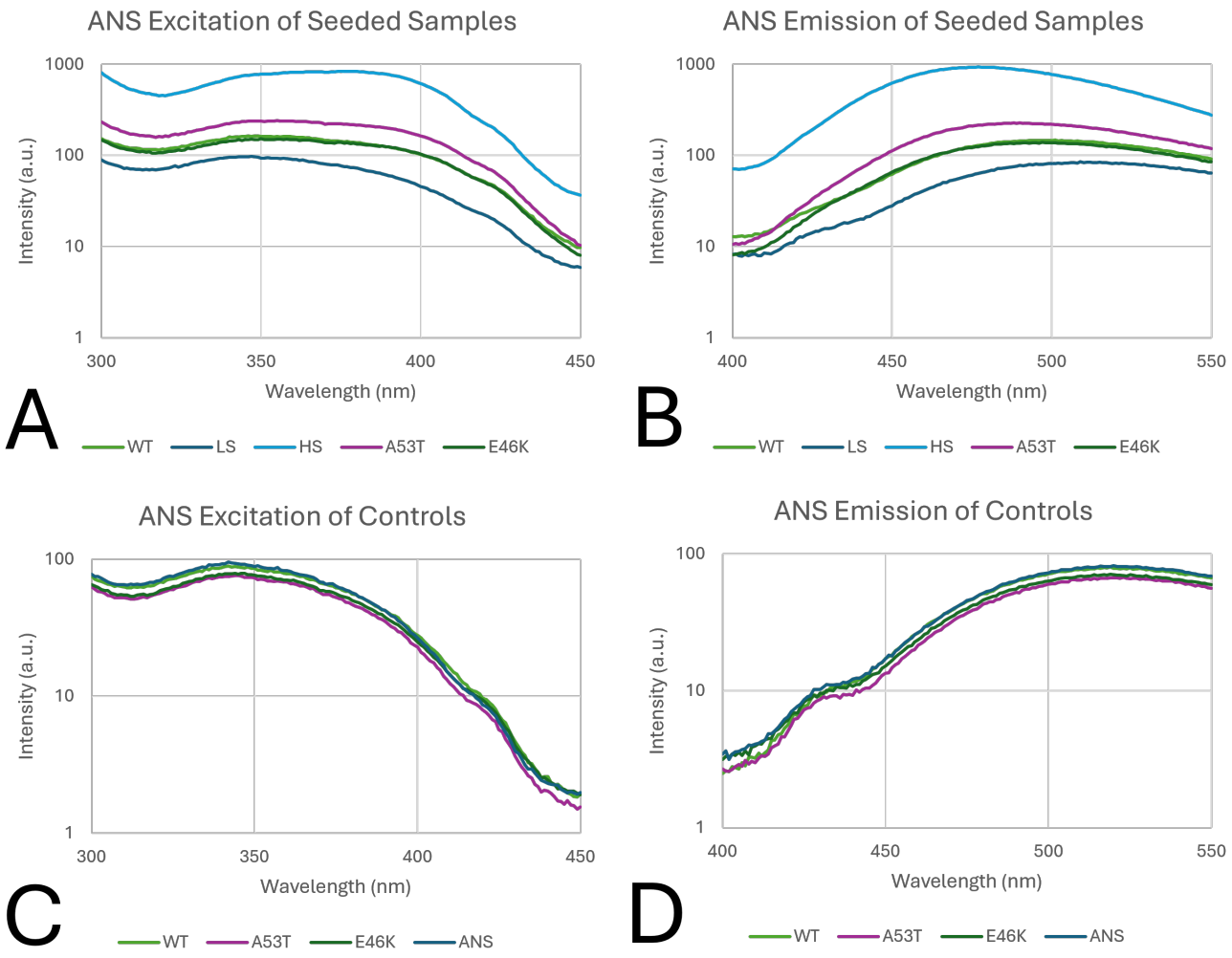

Figure 27 Excitation and emission spectra of seeded samples as well as controls dyed with ANS with log scale.Enter Caption

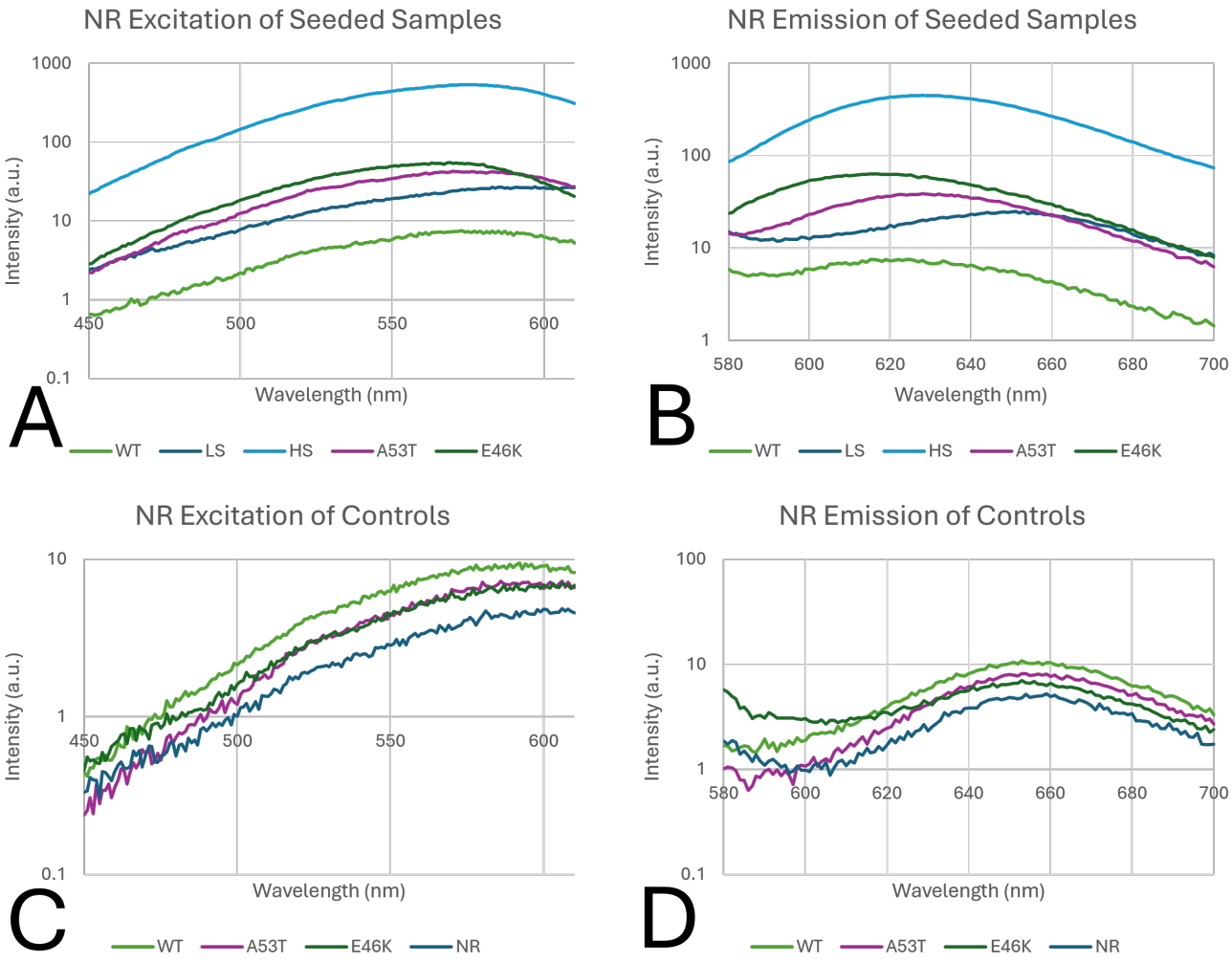

Figure 28 Excitation and emission spectra of seeded samples as well as controls dyed with NR with log scale.

5.6 Appendix F: Maxima of Controls

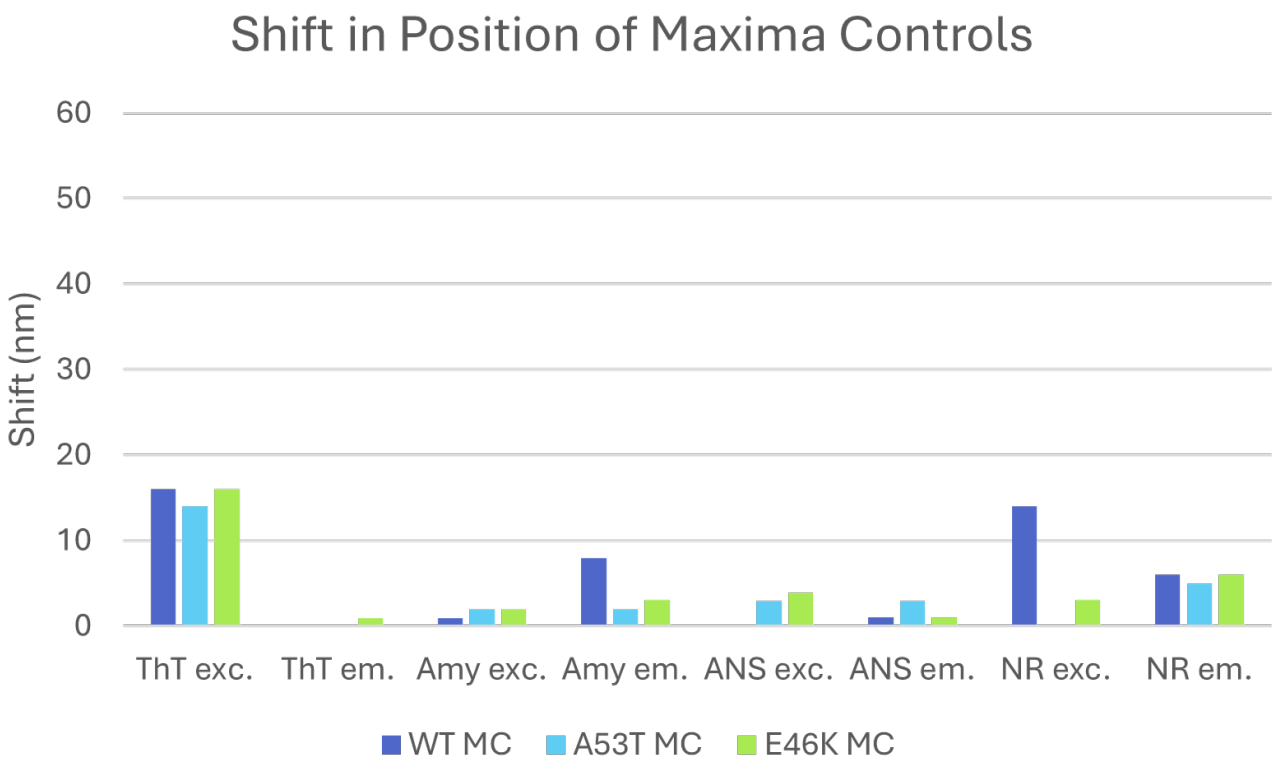

Figure 29 Shift in position of maxima compared to dye control grouped by dye and excitation/emission of controls.

5.7 Appendix G: AI Disclosure

AI has been used during the writing process of this report. During this, some lay-out suggestions from Chat-GPT such as the front page and table formatting have been incorporated, as well as spelling and grammar corrections by LanguageTool. This has been done only after careful consideration and reviewing.